Collapse of a Cavitation Bubble Near an Air Pocket

Changhwan Jang, Jihoo Moon, Ehsan Mahravan, and Daegyoum Kim

Abstract The dynamics of the cavitation bubble differ depending on the type of boundary near the bubble because the boundary affects the pressure distribution in the vicinity of the bubble. The asymmetric contraction speed of an interface of a collapsing cavitation bubble due to the asymmetric pressure distribution induces a high-speed bubble jet. The cavitation bubble near a rigid solid causes a bubble jet towards the solid surface during the bubble collapse, leading to cavitation erosion on the solid. Recently, a few studies have investigated a gas-entrapping microtextured surface to alleviate cavitation erosion. They confirmed that a bubble jet induced by a collapsing cavitation bubble near air in a pocket directs away from the surface, entrapping the air. In this study, we numerically investigate the hydrodynamic loading on a wall with an air pocket and the alleviation of cavitation erosion by the entrapped air on the solid surface. The presence of an air pocket mitigates the pressure on the wall during the bubble expansion and contraction. However, high pressure is still observed for a small distance between the air pocket and the bubble. The direction of the bubble jet also agrees well with the previous studies, and the tendency of the bubble jet direction is explained by the interaction of the cavitation bubble and the entrapped air in the pocket.

Keywords Cavitation bubble · Cavitation erosion · Air pocket

C. Jang · J. Moon · D. Kim (✉)
KAIST, Daejeon, Republic of Korea
e-mail: daegyoum@kaist.ac.kr

E. Mahravan
Aarhus University, Aarhus, Denmark

D. Kim et al. (eds.), *Fluid-Structure-Sound Interactions and Control*, Lecture Notes in Mechanical Engineering, https://doi.org/10.1007/978-981-97-6211-8_32

1 Introduction

A cavitation bubble is generated in a liquid due to low local pressure or high local temperature. The dynamics of the cavitation bubble depends on a type of adjacent boundary, such as a rigid wall, free surface, elastic wall, Etc. For this reason, cavitation bubble has many engineering applications (e.g., laser-induced forward transfer [1]).

A cavitation bubble causes a liquid jet during the collapse of the bubble. During the bubble contraction, the bubble interface does not shrink uniformly due to the asymmetric pressure distribution near the bubble. As a result, a liquid jet is induced at the interface of the collapsing cavitation bubble. Another noticeable feature of a cavitation bubble is the emission of a shock wave. In general, a cavitation bubble initially has much higher pressure than atmospheric pressure, leading the bubble to emit a shock wave.

The pressure near the hydraulic machinery, which operates with a fast motion in a liquid, decreases so that cavitation occurs near the surface of the machinery. If cavitation occurs near a solid surface, the bubble can cause undesirable noise, vibration, and surface erosion. These phenomena lead to inefficient energy performance and a high maintenance cost. Therefore, the mechanism of surface erosion due to a cavitation bubble has been studied for a long time. Cavitation erosion has several mechanisms depending on the stand-off parameter, which is the dimensionless distance between the inception location of the cavitation bubble and the solid surface [2]. The principal causes of the surface erosion by the cavitation bubble are the shock wave from the bubble and the high-speed liquid jet.

Recently, a few studies have been done to mitigate cavitation erosion by air cavities on the solid surface [3–5]. These studies commonly confirm that a bubble jet induced by a collapsing cavitation bubble near air cavities directs away from the solid surface with the cavities. From the direction of the liquid jet, the cavitation erosion is likely to be mitigated by the air cavity. However, the hydrodynamic loading on the solid surface with an air pocket and the dynamics of the air entrapped in the pocket still require further analysis.

In this study, we numerically investigate the hydrodynamic loading on the solid surface with an air pocket and the interaction of the cavitation bubble and entrapped air in a pocket by varying the geometry of the air pocket and the stand-off parameter. The elevation of the pressure on the surface due to the shock wave from the bubble decreases by the air entrapped in the pocket. Similar to the previous studies, the direction of the liquid jet induced by the collapsing bubble changes when there is an air pocket near the bubble.

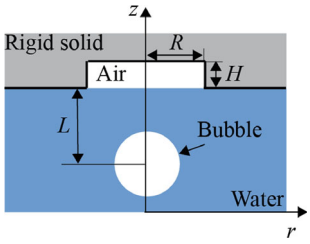

Fig. 1 Schematic of a bubble and air pocket on a rigid wall

2 Problem Description

2.1 Model and Parameters

This study considers a singular, cylindrical air pocket on a rigid wall and a bubble below the pocket with high initial pressure. For simplicity, the initial center of the bubble is on the axis of the cylindrical air pocket. In this condition, the flow can be treated as axisymmetric for the symmetric axis of the air pocket. The geometry of the air pocket is determined by the pocket radius R and the pocket depth H, so the dimensionless parameters $R^* = R/R_{unb,\max}$ and $H^* = H/R_{unb,\max}$ are treated as main parameters to vary the geometry of the air pocket, where $R_{unb,\max}$ is the maximum radius of the unbounded bubble during its expansion. The stand-off parameter $\gamma = L/R_{unb,\max}$ is also the main parameter, where L denotes the distance between the water–air interface and the inception of the bubble. In all cases, the initial bubble radius and initial bubble internal pressure are 4 μm and 147 MPa, respectively. $R_{unb,\max}$ is obtained by solving the Rayleigh-Plesset equation with the fourth-order Runge–Kutta method. $R_{unb,\max}$ is 60 μm under the initial bubble radius, pressure condition mentioned before (Fig. 1).

2.2 Numerical Methods

The numerical simulations are performed by a revised code from OpenFOAM. The compressible PISO algorithm is utilized to solve the governing equation of the fluid (Eqs. 1 and 2).

$$\frac{\partial \rho}{\partial t} + \nabla \cdot (\rho \boldsymbol{U}) = 0 \tag{1}$$

$$\frac{\partial (\rho \boldsymbol{U})}{\partial t} + \nabla \cdot (\rho \boldsymbol{U}\boldsymbol{U}) = -\nabla p + \rho \boldsymbol{g} + \nabla \cdot \boldsymbol{\tau} + \boldsymbol{f}_{surf} \tag{2}$$

ρ, $\boldsymbol{U}$, p, $\boldsymbol{g}$, $\boldsymbol{\tau}$, and $\boldsymbol{f}_{surf}$ denote fluid density, velocity, pressure, gravitational acceleration, viscous stress, and surface tension force per unit volume, respectively.

The gas inside the bubble and pocket are treated as steam and air, respectively. The whole domain is initially filled with water except for the inside of the bubble and the pocket. The volume of fluid (VOF) method captures the water–air and water-steam interface. The equation below is solved to obtain the volume fraction of each fluid α_i.

$$\frac{\partial \alpha_i}{\partial t} + \nabla \cdot (\alpha_i \boldsymbol{U}) + \nabla \cdot [\alpha_i (1 - \alpha_i) \boldsymbol{U}_r] = \alpha_i \left(-\frac{\psi_i}{\rho_i} + \sum_{k=1}^{3} \alpha_k \frac{\psi_k}{\rho_k} \right) \frac{Dp}{Dt} + \alpha_i \nabla \cdot \boldsymbol{U} \tag{3}$$

$\boldsymbol{U}_r$ is the relative velocity between the two phases, ψ is defined as $D\rho/Dp$, and D/Dt denotes a material derivative. The initial time step size is 0.01 ns, and the time step size changes to ensure that the Courant-Friedrichs-Lewy (CFL) number is below 0.1 at each time step.

The computational grid near the air and bubble consists of a uniform and fine grid by three times grid refinement (Fig. 2a.). After the grid refinement, the size of most fine grid Δx is 0.2 μm. To reduce the computational cost, the size of the grid exponentially increases as the distance from the region of interest increases. The grid convergence test results for verifying the grid size independence are shown in Fig. 2. N is the number of computational cells constructing the initial bubble radius. Δx is equal to 0.2 μm for $N = 20$. For $N \geq 20$, the maximum volume of air after its expansion converges with an error of less than 0.7% concerning $N = 40$. Therefore, the smallest grid size Δx is fixed as 0.2 μm ($N = 20$) in this study.

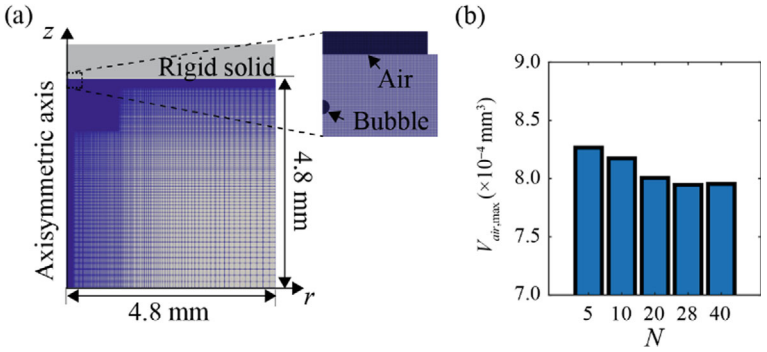

Fig. 2 **a** Axisymmetric two-dimensional computational grid for numerical simulations. **b** The maximum volume of air entrapped in the pocket with different grid sizes for $R^* = 1.0$, $H^* = 0.9$, $\gamma = 1.6$

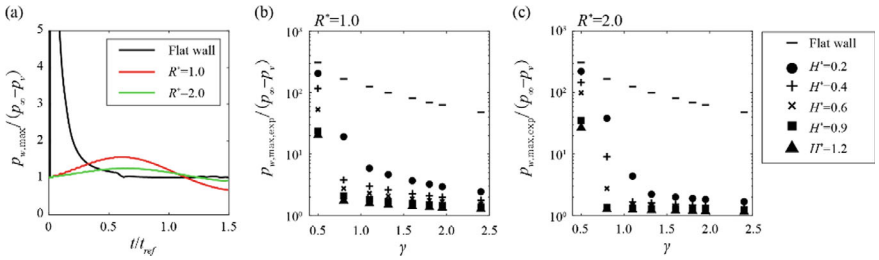

Fig. 3 **a** Spatial maximum pressure on the wall before bubble collapse for $H^* = 0.9$, $\gamma = 1.6$. Temporal maximum of $p_{w,\max}$ during the bubble expansion for **b** $R^* = 1.0$ and **c** $R^* = 2.0$. The subscription 'exp' denotes the bubble expansion

3 Results and Discussion

3.1 *Maximum Pressure on a Solid Surface During the Bubble Expansion*

First, the pressure mitigation effect of the presence of an air pocket is investigated. The spatial maximum pressure on the horizontal wall inside the pocket $p_{w,\max}$ is shown in Fig. 3a. p_∞ and p_v denote atmospheric pressure and vapor pressure of water, respectively. t_{ref} is defined as $R_{unb,\max}\{\rho/(p_\infty - p_v)\}^{1/2}$, where ρ is the density of the water. The peak of $p_{w,\max}$ at the beginning of the bubble expansion is due to the shock wave induced by the high initial pressure of the bubble for a flat wall. The entrapped air in a pocket reflects the shock wave at the water–air interface due to the much lower acoustic impedance of the air than that of the water. As a result, the pressure peak disappears for most of the air pocket cases.

The cause of the large pressure peak for the small stand-off parameter is the water collision with the wall (Fig. 3b, c). A small stand-off parameter means the bubble is close to the water–air interface. Consequently, the water–air interface collides with the wall during the bubble expansion, and it causes significant hydrodynamic loading on the wall.

3.2 *Direction of a Bubble Jet Near an Air Pocket*

The bubble jet induced by the collapsing cavitation bubble adjacent to an air pocket directs away from the pocket (Fig. 4). U_{ref} is defined as $R_{ubn,\max}/t_{ref}$. The reversed bubble jet direction can be explained by a similar mechanism of the bubble jet near a free surface. Because of the low inertia of the entrapped air, the upper interface of the bubble has faster motion during the bubble expansion and contraction. During the bubble contraction, the water is directed towards the bubble, which increases the pressure near the bubble. Due to the faster motion of the upper interface of the bubble,

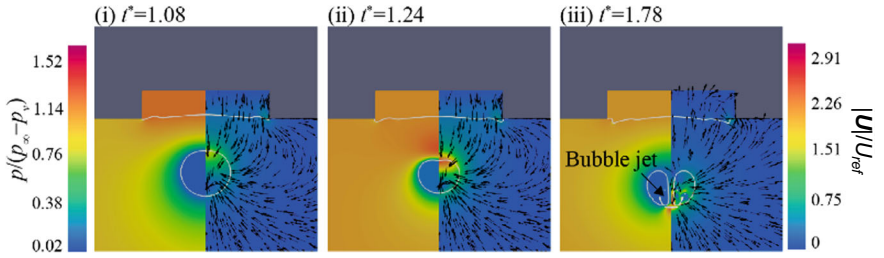

Fig. 4 Formation of a bubble jet for $R^* = 2.0$, $H^* = 0.9$, $\gamma = 1.6$

a higher pressure region appears above the bubble, and it accelerates downwards the bubble's upper interface during the bubble collapse. Consequently, the bubble jet is directed away from the air pocket.

4 Concluding Remarks

In this study, we investigate the the alleviation effect of hydrodynamic loading on a wall by an air pocket. The high-pressure peak at the beginning of the bubble expansion is because of the shock wave, and the pressure peak disappears for air pocket cases. However, if the bubble is too close to the water–air interface, the bubble expansion causes a water collision with the wall, leading to a high pressure similar to the flat wall cases. The bubble jet near an air pocket directs away from the air pocket, and the high pressure due to the bubble jet disappears by the presence of the entrapped air in the pocket. The reversed direction of the bubble jet is explained by the interaction of the bubble and the entrapped air.

References

1. Mahravan E, Kim D (2021) Bubble collapse and jet formation inside a liquid film. Phys Fluids 33(11)
2. Philipp A, Lauterborn W (1998) Cavitation erosion by single laser-produced bubbles. J Fluid Mech 361:75–116
3. Gonzalez-Avila SR, Nguyen DM, Arunachalam S, Domingues EM, Mishra H, Ohl C (2020) Mitigating cavitation erosion using biomimetic gas-entrapping microtextured surfaces (GEMS). Sci Adv 6:13
4. Sun Y, Du Y, Yao Z, Zhong Q, Geng S, Wang F (2022) The effect of surface geometry of solid wall on the collapse of a cavitation bubble. J Fluids Eng 144(7)
5. Sun Y, Yao Z, Wen H, Zhong Q, Wang F (2022) Cavitation bubble collapse in a vicinity of a rigid wall with a gas entrapping hole. Phys Fluids 34(7)